Insights into the catalytic promotion of propylene self-metathesis over silica-supported molybdenum oxide using substituted olefins.

Ran Zhu,[1] Husain H. Adamji,[1] Zachariah J. Berkson,[2, 3] Jie Zhu,[1] Ashley R. Head,[4] Heather J. Kulik,[1] Christophe Copéret,[2] and Yuriy Román-Leshkov[1*]

[1] Department of Chemical Engineering, Massachusetts Institute of Technology (MIT), Cambridge, MA 02139, USA
[2] Department of Chemistry and Applied Bioscience, ETH Zürich, Zürich, Switzerland
[3] School for Engineering of Matter, Transport and Energy, Arizona State University, Tempe, Arizona 85287, USA
[4] Center for Functional Nanomaterials, Brookhaven National Laboratory, Upton, NY 11973, USA

[*]: yroman@mit.edu

Abstract:

Olefin metathesis is a versatile strategy for functional group interconversion around C=C bonds. Here, we investigate in detail a recently discovered promotional effect, where co-feeding 2,3-dimethyl-2-butene isomers (4MEs) increases propylene self-metathesis rates on silica-supported Mo and W oxides by orders of magnitude. Through detailed kinetic measurements on MoO_x/SiO_2, we validate a dynamic site renewal and decay cycle, analogous to WO_x/SiO_2, which operates in tandem with the Chauvin cycle and can be effectively modulated by co-feeding 4MEs. Active site titrations indicate that the promotional effect results from an increased density of active sites rather than enhanced per-site catalytic activity. Spectroscopic analyses reveal that the renewal and decay of Mo alkylidene active sites involve proton-transfer mediated by proximal acidic Si-OH groups. Additionally, the co-fed promoters not only reduce Mo (VI) to Mo (IV), thereby increasing the number of pre-active sites, but also act as proton relays, enhancing proton-transfer steps. This dual functionality elucidates the mechanism underlying the enhanced metathesis activity observed with promoter addition.

Introduction

Olefin metathesis plays an important role in both industrial processes and fundamental research due to its high atom-economy, negligible non-olefin products, and broad utility ranging from fine chemical synthesis to large-scale production of commodity chemicals.[1-3] It is widely accepted that heterogeneous olefin metathesis shares the Chauvin mechanism with its homogeneous counterpart, involving metal alkylidene and metallacyclobutane intermediates.[4,5] However, the detection of alkylidene moieties is elusive.[6,7] It has been hypothesized that the active sites form in-situ from isolated metal-oxo and/or metal-dioxo precursor surface species upon interaction with the olefin substrate at elevated temperatures.[4,8,9] Despite extensive industrial use and research on the topic, the detailed mechanisms governing the formation and decay of active sites on supported metal (W, Mo, Re) oxide catalysts are still poorly understood.[3,9] Furthermore, the kinetically and

thermodynamically demanding nature of such an activation process[8,9] results in a very low fraction of catalytically active metal centers, consistent with the low intrinsic mass activity of industrial Mo- and W-based heterogeneous catalysts and the lack of detectable spectroscopic signatures of these reaction intermediates.[4,10]

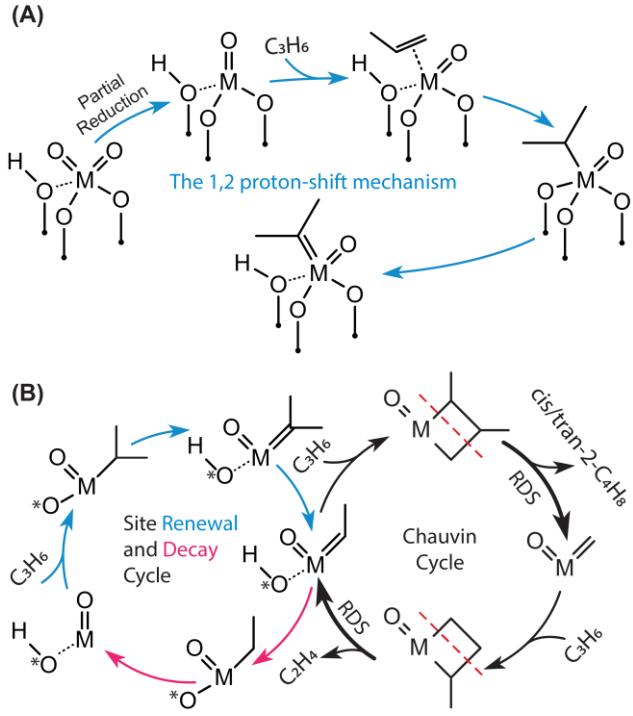

Figure 1. (A) the 1,2-proton shift mechanism on partially reduced supported metal (Mo or W) oxides, and **(B)** Active site renewal and decay cycle through 1,2-proton shift mechanism, where *O is a lattice oxygen of the support and M is the metal center. RDS stands for rate-determining step.

Based on transient and steady state kinetic measurements, our recent study extended the Chauvin cycle for supported metal oxide catalysts, proposing that active sites for propylene self-metathesis on WO_x/SiO_2 undergo a dynamic site decay and renewal cycle **(Fig. 1B)** following a 1,2-proton shift mechanism **(Fig. 1A)**.[11-13] This proposed dual cycle explains the experimentally observed higher propylene and 2-butene orders than those predicted by the traditional Chauvin cycle. Additionally, co-feeding metathesis-inert substituted olefins, such as 2,3-dimethyl-1-butene (i-4ME) that do not readily undergo metathesis, resulted in a 30-fold increase in propylene self-metathesis rates at 250 °C on WO_x/SiO_2 catalysts with minimal promoter consumption. We proposed that i-4ME facilitates proton transfer in the 1,2-proton shift mechanism, thereby increasing and allowing the regeneration of the active site count during the promoted steady state. However, direct evidence for increased active site density has remained elusive, primarily due to the short-lived nature of these sites under typical reaction conditions. Furthermore, while our findings also confirmed the promotional effect on MoO_x/SiO_2, akin to WO_x/SiO_2, detailed kinetic and spectroscopic analyses to confirm whether the promotional effects on MoO_x/SiO_2 and WO_x/SiO_2 are analogous remained to be investigated.

Here, we investigate the kinetic and thermodynamic effects of promotion resulting from co-feeding 2,3-dimethyl-2-butene isomers (4MEs) on olefin metathesis using monodispersed MoO_x/SiO_2 catalysts prepared via surface organometallic chemistry.[14] We observed an increase in propylene self-metathesis rates by 44-77 fold and 3-6 fold for cross-metathesis of 2-butenes and ethylene under various conditions. Kinetic studies for both self- and cross-metathesis elucidated the impact of 4MEs on the apparent activation energy and reaction orders for olefins and 4MEs. Steady state transient active site titration revealed an increase in Mo ethylidene density by almost one order of magnitude, from 2.8×10^{-5} mol/g_{cat} to 12.1×10^{-5} mol/g_{cat} under 20% 2-butenes with 1% co-fed 4MEs. This increase closely matches the enhanced steady-state rate observed in 2-butenes and ethylene cross-metathesis. Spectroscopic analysis supports that the promotional effect of co-fed 4MEs primarily stems from an increased active site quantity, facilitated by the 1,2-proton shift

mechanism. In this mechanism, 4MEs act both as a proton shuttle and a reductant, converting Mo(V/VI) to Mo(IV), which is extensively proposed as the pre-active site for Mo alkylidenes.[4,15,16]

Results:

Kinetics of self- and cross-metathesis on MoO_x-SOMC

We investigated the kinetics of propylene self-metathesis and cross-metathesis of ethylene and 2-butenes using a 1.5 wt. % Mo loading MoO_x/SiO_2 catalyst, synthesized via a surface organometallic chemistry approach (1.5% MoO_x-SOMC).[14,17,18] This catalyst predominantly features isolated, monodispersed Mo-dioxo species on silica,[17] eliminating the potential complications from metal clusters or interface sites found in catalysts prepared by traditional incipient wetness impregnation methods.[14] To verify the broad applicability of our findings, we conducted comparative analyses with a 6.6% Mo loading MoO_x/SiO_2 catalyst prepared via incipient wetness impregnation (6.6% MoO_x-IWI). This catalyst, comprising mono-molybdates, poly-molybdates, and MoO_3 crystalline clusters, represents typical industrial supported catalysts, as reported in prior literature.[19] The kinetics were measured under differential conditions, free from mass and heat transport limitations **(Supplementary Eq. S1-S4)**. In the absence of promoter olefin, the 1.5% MoO_x-SOMC exhibited an apparent propylene order of 1.4 and an apparent activation energy (E_{app}) of 53 kJ/mol **(Fig. 2A and B)**. The propylene order, exceeding the previously reported range of 0.78-0.84 on MoO_x/Al_2O_3 and surpassing the predicted order of less than one

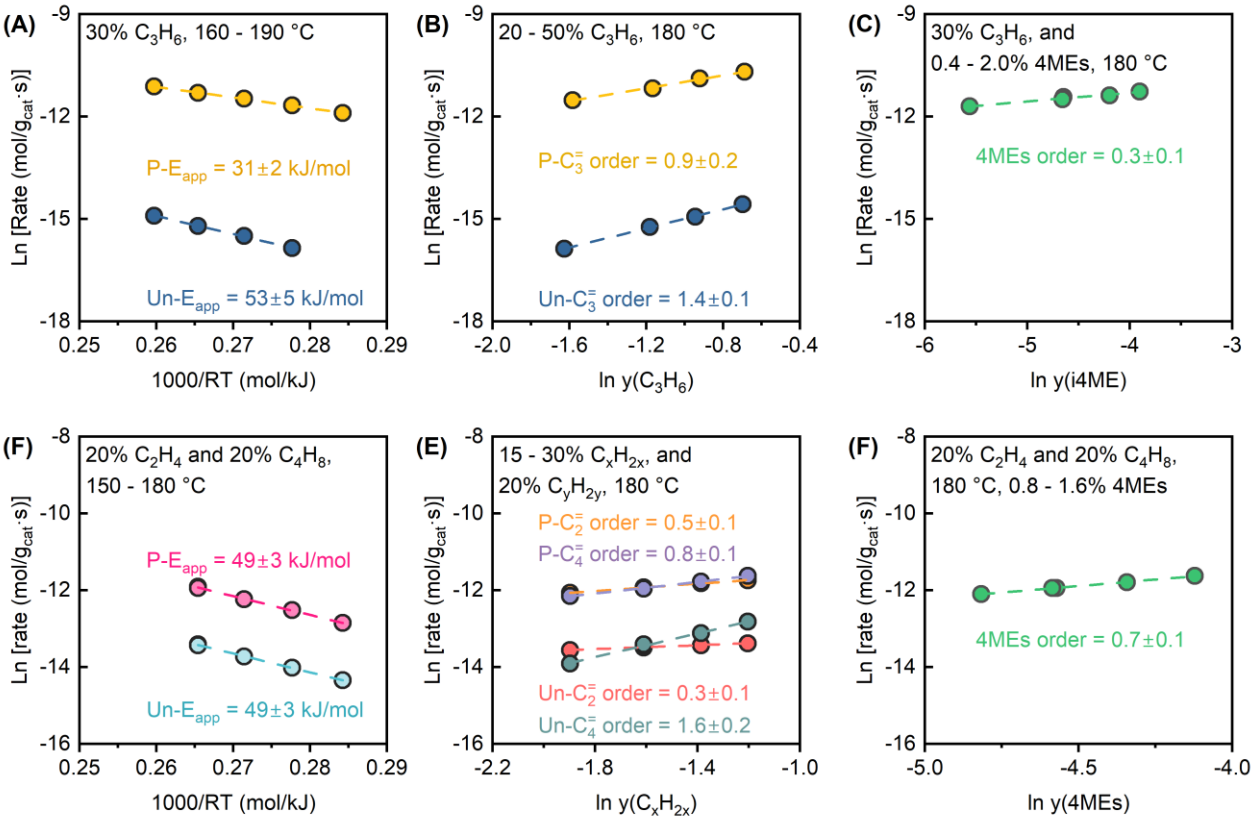

Figure 2. Kinetic parameters for olefin metathesis over 1.5%MoO_x-SOMC. **(A)** Arrhenius plots of propylene ($C_3^=$) metathesis, **(B)** $C_3^=$ order, **(C)** 4MEs order, **(D)** Arrhenius plots of ethylene ($C_2^=$) and 2-butenes ($C_4^=$) cross metathesis, **(E)** $C_2^=$ and $C_4^=$ orders, and **(F)** 4MEs order. Promotions in **(A)**, **(B)**, **(F)**, and **(E)** are performed by co-feeding 1.0 mol % 4MEs. P- for promoted conditions and Un- for unpromoted conditions. Conditions: 15 mg catalyst, helium balanced 50 mL/min total flow.

from the Chauvin cycle,[20] hints at kinetically relevant steps on MoO_x/SiO_2 beyond the traditional Chauvin cycle. In the cross-metathesis of 2-butenes and ethylene, our measurements indicated an ethylene order of 0.3, a 2-butenes order of 1.6, and an E_{app} of 49 kJ/mol **(Fig. 2D and E)**. These results align with our previous observations on the 3% WO_x-SOMC catalyst,[11] suggesting the presence of a site renewal and decay cycle. The notably higher order of 2-butenes order, at 1.6, comparable to the order of propylene (1.4) in propylene self-metathesis, versus the lower ethylene order of 0.3, implies that 2-butenes are likely involved in kinetically relevant steps that do not include ethylene. A plausible explanation is that 2-butene, like propylene, more effectively participates in the site renewal and decay cycle, thus predominantly sustaining active sites in an equimolar cross-metathesis system.

Although pure i-4ME was co-fed as the promoter into the reactor, we observed that after passing through the moisture and oxygenates traps, a mixture of i-4ME and its isomer, 2,3-dimethyl-1-butene (n-4ME), was detected before the reactor inlet **(Supplementary Table S2)**.[21] Thus, the promoters entering the reactor comprised a mixture of i-4ME and n-4ME, collectively referred to as 4MEs. Control experiments revealed that the propylene self-metathesis rate reached a promoted steady state within 5 hours of introducing 1% 4MEs and reverted to the original rate within ca. 20-50 hours after discontinuing the promoter **(Supplementary Fig. S1)**. This behavior suggests that 4MEs do not irreversibly alter the active sites. The presence of 1% 4MEs resulted in a 44-77 fold increase in the propylene self-metathesis rate under various conditions, accompanied by a reduction in the E_{app} to 31 kJ/mol, a decrease in the apparent propylene order to 0.9, and the establishment of a 4MEs order of 0.2 **(Fig. 2A-C)**. Similarly, in the cross-metathesis of ethylene and 2-butenes, the rate increased by 3 to 6-fold under different conditions. The promoted order for 2-butenes decreased to 0.8, aligning closely with the ethylene order of 0.5, with an apparent 4MEs order of 0.7 **(Fig. 2D-F)**. These findings show that co-fed 4MEs modify the kinetic dependence of propylene and 2-butenes within the site renewal and decay cycle, reducing their apparent orders to align with the 0-1 range predicted by the Chauvin cycle.

Promotional effect on active site density

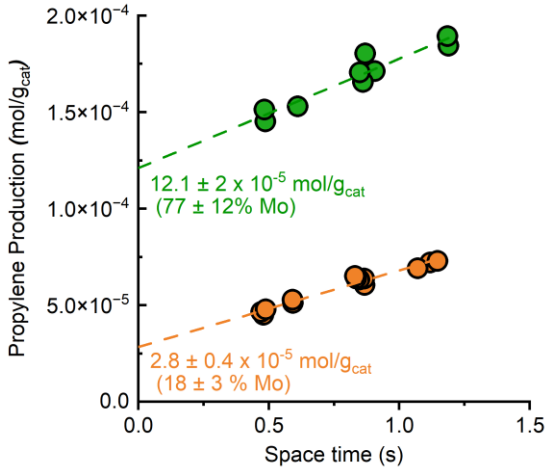

Figure 3. Propylene production during transition from 20% 2-butenes to 20% ethylene with (green) and without (orange) 1% 4MEs co-feeding. Conditions: 30 mg catalyst, helium balanced, 40 to 90 mL/min total flow rate at 180 ºC.

The promotional effect on active site density was assessed by titrating the quantity of active sites, presumed to be Mo oxo ethylidenes, at steady state under 20% 2-butenes **(Methods)**. We performed this titration on the 1.5% MoO_x-SOMC catalyst by switching from 20% 2-butenes to 20% ethylene using a steady-state isotopic transient kinetic analysis (SSITKA) reactor **(Supplementary Fig. S4)** under differential conditions. Extrapolating propylene production at various space times to 0 space time indicated a production of $2.8 \pm 0.4 \times 10^{-5}$ mol/g_{cat}, which corresponds to an equivalent Mo oxo ethylidene count, suggesting that 18 ± 3% of surface Mo is catalytically active **(Fig. 3)**. The addition of 1% 4MEs resulted in a substantial increase in Mo oxo ethylidene density. Specifically, the density of catalytically active surface Mo on our catalyst

increased 4.3-fold to 12.1 ± 0.4 × 10^{-5} mol/g_{cat}, amounting to 77 ± 12% of the total surface Mo. This value significantly exceeds the previously reported maximum of ca. 20% for supported metal oxides.[4,22-24] The increasing trend in active site density while co-feeding 1% 4MEs was consistent across catalysts with 1.4% and 6.6% MoO_x-IWI, as well as 2.9% WO_x-IWI catalysts **(Supplementary Fig. S5)**. This trend correlates closely with the observed 4.5-fold increase in the rate of cross-metathesis between ethylene and 2-butenes under similar conditions (**Fig. 2F**). The corresponding 4.3-fold increase in active site density, as indicated by active site titration, directly implies that this increase is the principal factor influencing the promotional effect on the steady state rate of olefin metathesis.

The formation of metathesis-active metal alkylidene sites on fully oxidized supported metal oxides typically involves two steps: an initial reduction that removes an oxo ligand from a surface metal(VI) dioxo site, followed by a reaction between the resulting partially reduced metal site and an olefin to form an alkylidene.[9,16,25] We posit the promotional effect could enhance active site density by either reducing additional surface Mo(VI) species to Mo(IV) or by facilitating metal alkylidene formation. A recent study using solid-state ^{95}Mo NMR and reactivity tests on a SOMC-derived Mo oxide catalyst with high surface area (2.3% MoO_x-$SOMC_{HSA}$) identified ca. 22% of Mo sites in a strained tetrahedral SiO–$Mo(=O)_2$–OSi configuration (denoted Site I).[17] Site I is characterized by a small O-Mo-O angle of ca. 90°, with low LUMO (Least Unoccupied Molecular Orbital.) energies and high reducibility, and thus proposed to be the most effective pre-active sites for metal alkylidenes.

This study, in synthesizing the 1.5% MoO_x-SOMC, has maintained consistency of synthesis conditions, surface Mo densities (0.47-0.48 Mo/nm²), and Mo loading-normalized site time yields for promoted and unpromoted propylene self-metathesis, to permit fair comparisons. Indeed, for 1.5% MoO_x-SOMC, 18% of surface Mo sites are active under unpromoted conditions, in good agreement with the ratio of Site I in previous work. The 77% of active surface Mo under promoted conditions suggests that co-fed 4MEs may reduce Mo sites with lower reducibility than Site I, potentially generating additional Mo(IV) pre-active sites during the induction period of promotion in metathesis.

In-situ reduction of surface Mo during the promotion

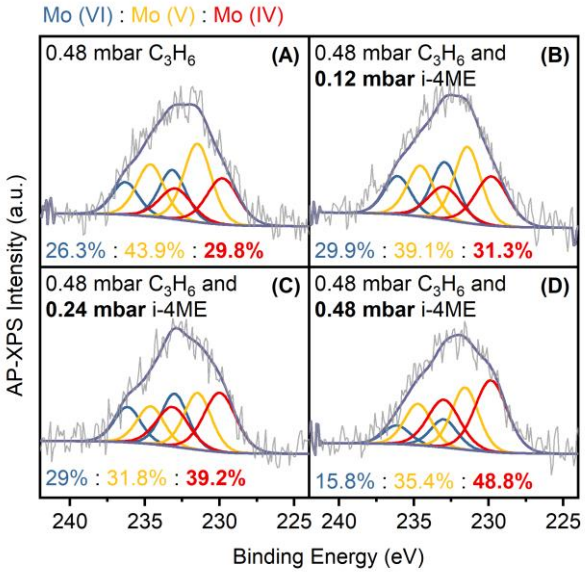

Figure 4. (A)–(D) NAP-XPS data of the Mod 3d region of the 1.5% MoO_x-SOMC catalyst subject to conditions labeled in the spectra at 250 ºC. The fitted peaks for Mo (VI) are blue, Mo (V) are yellow, and Mo (IV) are red. Parameters used in peak deconvolution are listed in the Supplementary Table S3.

The reduction of surface Mo by 4MEs was examined using near-ambient pressure X-ray photoelectron spectroscopy (NAP-XPS). The Mo 3*d* region of the XPS data showed peaks corresponding to Mo $3d_{5/2}$ and Mo $3d_{3/2}$ for each oxidation state of Mo **(Fig. 4)**. After exposing the pretreated catalyst pellet to 0.48 mbar of propylene, we observed the distribution of surface Mo **(Fig. 4A)** to be 26.3% Mo (VI), 43.9% Mo (V), and 29.8% Mo (IV). Next, increasing the i-4ME pressure in the analysis chamber **(Fig. 4)** led to a monotonic increase in the proportion of Mo (IV) from 29.8% to 48.8%, while the proportions of Mo (VI) and Mo (V) decreased. Note that the reduction by i-4ME could occur on fully oxidized Mo (VI) dioxo sites or other Mo (VI) sites bonded with organic species. However, the absence of oxygenates in the reactor effluent during catalytic studies introduces uncertainty regarding the specific reduction mechanism. The reduction of surface Mo by 4MEs, under similar conditions to our reactivity studies, was also investigated using in-situ diffuse reflectance (DR) UV-Vis spectroscopy, focusing on changes in the d-d electron transitions of surface Mo cations. Strong adsorption bands were observed between 300 and 700 nm upon co-feeding 1% 4MEs during steady-state propylene self-metathesis **(Supplementary Fig. S7)**. However, the presence of reduced surface Mo sites could not be definitively identified due to overlapping π-π* electron transitions that produce features in the same spectral region.[26-28]

The observed increase in Mo (IV) ratios with increasing i-4ME partial pressures suggests that i-4ME facilitates the reduction of surface Mo to Mo (IV). This Mo (IV) form, primarily existing as an oxo structure, is hypothesized to be a pre-active site that reacts with olefins to form metathesis active species, presumably Mo oxo alkylidenes.[13,15,16,29] Therefore, the i-4ME-induced increase in Mo (IV) ratios may lead to an increase in the number of metathesis-active Mo alkylidene sites, suggesting that the promotional effects of 4MEs co-feeding are due in part to the enhanced reduction of surface Mo. This hypothesis is supported by previous studies, which have shown a correlation between metathesis activity and the reducibility of supported metal oxides.[17,30-32]

Next, we investigated if factors other than reducibility contributed to the promotional effect. It has been reported that high temperature pretreatments under olefins or alkanes can promote the steady state rate of olefin metathesis over supported metal oxides by reducing the surface metal oxides.[23,32,33] We thus examined the promotional effect of 4MEs on the 1.5% MoO_x-SOMC catalyst activated under 4% propylene at 550 °C for 30 mins.[23] Such pretreatment minimizes further reduction of Mo by 1% 4MEs at 180 °C. Nonetheless, we observed that introducing 1% 4MEs to the propylene-activated catalyst still induced a promotional effect (1.1 to 1.3 fold), albeit less pronounced than on a catalyst activated under helium **(Supplementary Fig. S8)**. This result

suggests that the role of 4MEs in promoting catalytic activity extends beyond merely enhancing the reduction of Mo as proposed earlier (see below).

Surface proton-transfer during the promotion

In-situ transmissive Fourier-transform infrared (FTIR) spectroscopy was employed to study the interactions of the pretreated 1.5% MoO_x-SOMC catalyst with either propylene or 4MEs by separately exposing the catalyst surface to 10% propylene or 1% 4MEs at 50 °C. The absorbance differences in the resulting spectra compared to the fresh catalyst **(Fig. 5)** revealed changes on the catalyst surface following the adsorption of these probe molecules. For the propylene-saturated catalyst **(Fig. 5A, orange trace)**, limited changes were observed. The spectra primarily displayed features due to sp^3 C-H stretching (2800 to 3050 cm^{-1}) and a negligible decrease in the Si-OH (3747 cm^{-1}) feature.[34] Weak peaks at 2984 cm^{-1}, 2936 cm^{-1}, and 2874 cm^{-1} were attributed to asymmetric sp^3 C-H stretching of primary and secondary carbons, and symmetric sp^3 C-H stretching, respectively.[35]

The adsorption of 4MEs onto 1.5% MoO_x-SOMC **(Fig. 5A, blue trace)** resulted in pronounced changes in the IR features, particularly in the isolated Si-OH feature at 3747 cm^{-1}, which was decreased in intensity significantly greater than that observed with propylene. Additionally, two types of perturbed Si-OH groups emerged at 3705 cm^{-1} and 3517 cm^{-1}.[36,37] With an integrated molar extinction coefficient (IMEC, ε) of 1.2-1.6,[38] the isolated Si-OH consumption post 4MEs adsorption was estimated at 22 ± 3 $\mu mol/g_{cat}$ **(Supplementary Fig. S9)**. The intense peaks in the 2800-3050 cm^{-1} region, corresponding to sp^3 C-H stretching, suggest various 4MEs adsorption modes on the catalyst surface. A control experiment with 4MEs on a $SiO_{2\text{-}700}$ support, dehydroxylated at 700 °C **(Fig. 5A, red trace),** showed similar perturbed Si-OH groups at 3708 and 3484 cm^{-1}, but minimal isolated Si-OH consumption (2.6 ± 0.4 $\mu mol/g_{cat}$), indicating that Si-OH consumption on 1.5% MoO_x-SOMC is not due to these perturbed Si-OH groups. Further, titration with CD_3CN revealed a strong peak at 2304 cm^{-1} on 1.5% MoO_x-SOMC, attributed to CD_3CN adsorbed on Brønsted acidic sites **(Supplementary Fig. S10 and Table S5)**.[39] This is consistent with our previous findings from a ^{15}N-labeled pyridine adsorption study, which detected ^{15}N-pyridinium formed at room temperature on the same catalyst.[11] These results imply that Si-OH consumption on 1.5% MoO_x-SOMC primarily results from the protonation of adsorbed 4MEs at Brønsted acidic Si-OH sites. The acidity of these Si-OH groups, together with surface temperature, likely determines the formation of either a

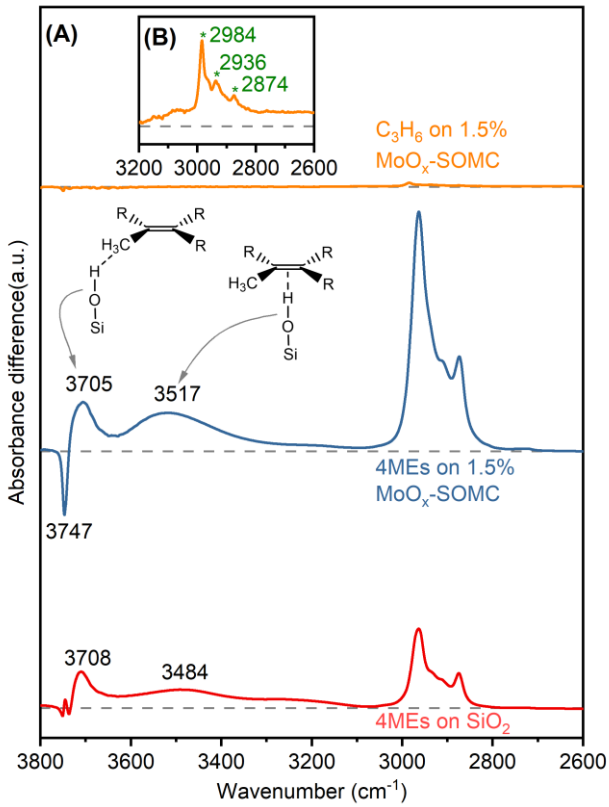

Figure 5. (A) In-situ transmissive FTIR spectra of the adsorption of C_3H_6 and 4MEs on 1.5%MoO_x-SOMC, and 4MEs on SiO_2 support at 50 °C. **(B)** A zoomed in version of C_3H_6 on 1.5% MoO_x-SOMC focusing on the C-H stretching region. The absorbance difference was relative to the fresh catalyst after pretreatment.

surface alkoxide or a surface alkyl species with a tertiary carbocation bound to the surface Si-O^- group.[40]

The increased consumption of Brønsted acidic Si-OH groups by 4MEs compared to propylene suggests a more extensive coverage by surface carbocations or alkoxides derived from 4MEs. This enhanced coverage is likely due to the higher boiling points of 4MEs and the electron-donating methyl groups attached to the alkene functionality in 4MEs, which stabilize the corresponding carbocations or alkoxides. While most surface-bound 4MEs desorbed from the catalyst above 180 °C **(Supplementary Fig. S11)**, we hypothesize that similar interactions persist on partially reduced Mo(IV) oxo surfaces under reaction conditions at 180 °C. Indeed, the elevated temperature at reaction conditions facilitates the desorption of 4MEs through deprotonation, establishing a dynamic adsorption-desorption cycle of 4MEs upon continuous co-feeding of 4MEs. During this cycle, the acidic protons transition between the Si-OH and the adsorbed 4MEs, positioning 4MEs as a potential proton shuttle. These labile protons, generated from the desorption of 4MEs, can then protonate surface species adsorbed on nearby Mo.

Among the various mechanisms proposed for the transition from metal dioxo to metal alkylidene, proton transfer is the key step in the well-documented 1,2-proton shift mechanism.[41,42] Recent studies of homogeneous Mo and W organometallic complexes suggest that proton transfer from the surrounding proton donors to styrene interacting with the Mo and W complex is the rate-determining step for the formation of the corresponding metal alkylidene.[12,43,44] In addition, computational analysis indicates that the barriers for proton transfers from perturbed Si-OH to adsorbed propylene on Mo(IV) oxide and from the Mo isopropyl complex to the oxygen in the Mo-O-Si bond bridge correspond to the highest barriers in the energy landscapes for Mo oxo propylidene formation.[45] From these insights, we infer that the desorption of 4MEs through deprotonation of surface carbocations/alkoxides, producing labile protons, can facilitate the rate-determining proton transfer in the active site formation process, enhancing the generation of Mo alkylidenes. The increased quantity of Mo alkylidenes leads to a higher promoted steady state rate of propylene self-metathesis. Upon stopping 4MEs co-feeding, the site renewal and decay cycle likely transitions to a new state similar to the initial unpromoted steady state, resulting in a post-promotion steady state propylene self-metathesis rate similar to the initial unpromoted one.

Site renewal and decay cycle in addition to the Chauvin cycle

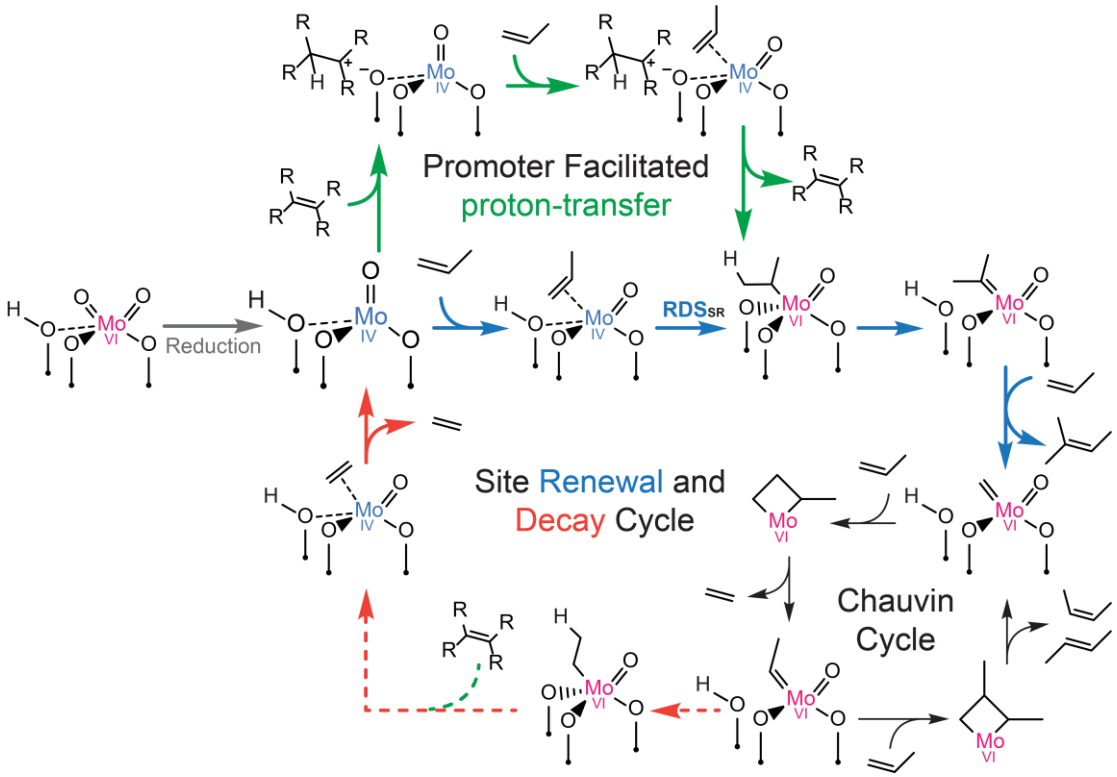

Figure 6. Proposed reaction mechanism for propylene self-metathesis over MoO_x/SiO_2. RDS_{SR} is the proposed rate determining step for the forward unpromoted 1,2-ptoton shift mechanism.

Drawing upon our kinetic and spectroscopic insights, we propose a mechanism for olefin metathesis **(Fig. 6)**, exemplified by propylene self-metathesis, that integrates a partial reduction, a site renewal and decay cycle, and the Chauvin cycle. The mechanism starts with the partial reduction of fully oxidized Mo (VI) dioxo to Mo (IV) which is detected by our AP-XPS measurements and has been extensively proposed as the pre-active site for catalysts activated under inert gas.[13,14,33] After the partial reduction, we propose the 1,2-proton shift mechanism as the site renewal pathway, complemented by a possible decay pathway via alkylidene protonation,[43,44] to account for the dynamic balance governing the surface coverage of Mo alkylidene. In this fashion, propylene coordinates at Mo (IV) oxo sites, leading to the formation of Mo alkylidene through multiple proton-transfer steps that involve the acidic proximal Si-OH group adjacent to the Mo species.[11,46] Once formed, the Mo alkylidene enters the Chauvin cycle thus producing ethylene, cis-, and trans-2-butenes. Within the Chauvin cycle, the Mo oxo ethylidene could undergo a proton-transfer to produce an ethylene and pre-active site, the Mo mono-oxo structure, closing the site renewal and decay cycle. Control experiments were conducted to investigate the site decay period **(Supplementary Fig. S3A)**. Step changes from 30% propylene in helium to pure helium and then back to 30% propylene resulted in negligible changes in the deactivation profile, suggesting that site decay is not kinetically dependent on propylene.

The nearly identical increase in active site count and the cross-metathesis rate of 2-butenes and ethylene upon 4MEs co-feeding, alongside the minimal metathesis reactivity of 4MEs, points to their influence on the site renewal and decay cycle rather than a direct effect on the Chauvin cycle. AP-XPS results suggest that 4MEs assist in the reduction of inactive surface Mo (V/VI), forming

pre-active Mo (IV) sites. However, the detailed mechanism of this reduction remains speculative. It might occur on fully oxidized Mo dioxo structures that possess high reducing potentials, or on surface intermediates like Mo (VI) oxo alkyl species. The inability of propylene alone to achieve promoted steady-state rates post-reduction implies that the promoter interacts with the newly reduced sites beyond just reduction. Therefore, we suggest that the 4MEs participate in a reaction pathway inaccessible to propylene which converts the pre-active Mo (IV) mono oxo site, reduced by 4MEs, into an active site. Such a pathway should be associated with the aforementioned proton-transfer steps.

Based on observations from in-situ FTIR, we propose a new site renewal pathway starting with the protonation of adsorbed 4MEs on partially reduced Mo (IV) oxo, forming surface carbocations or alkoxides. The subsequent desorption of these adsorbates can protonate neighboring adsorbed propylene on the Mo (IV) center, forming a Mo oxo isopropyl structure. A subsequential proton transfer and electron rearrangement leads to the formation of Mo alkylidene, which then initiates olefin metathesis. In the site renewal process, the adsorption and desorption cycle of 4MEs produces labile protons, catalyzing the forward reaction by facilitating the rate-determining step of the 1,2-proton shift mechanism in the site renewal and decay cycle. Notably, the renewal of sites pre-existing before reduction by 4MEs could also benefit from the promoted pathway. The rate exhibits a sub-first order dependence on the promoter, indicating that even within the promoted pathway, the site renewal and decay cycle likely does not reach equilibrium. A slight increase in the deactivation post-promotion was observed in the presence of 4MEs, suggesting that 4MEs may also promote the site decay pathway **(Supplementary Fig. S3C)**.

In-situ DR UV-Vis spectroscopy revealed prominent features (300 to 700 nm) during 4MEs co-feeding, suggesting the formation of surface aromatic complexes through possible aromatization over acid sites,[23,47] potentially acting as a carbon pool.[48,49] Despite the apparent stability of this carbon pool as seen in UV-Vis during the deactivation period of propylene self-metathesis post 4MEs co-feeding, the possibility for a proton-transfer promotion mechanism involving this carbon pool is not discarded.[50] The promotional effect was also evaluated on MoO_x-IWI catalysts with varying Mo contents (1.4 to 14.2 wt.% Mo), each showing varying degrees of increase in steady state propylene self-metathesis rates **(Supplementary Fig. S15)**. Notably, the extent of the promotional effect showed an inverse correlation with Mo loading, except for the 14.2% MoO_x-IWI. Efforts are ongoing to understand how Mo dispersion, reducibility, and Brønsted acidity influence the promotional effect.

Conclusion:

This comprehensive kinetic and spectroscopic study elucidates the origins of heterogeneous olefin metathesis promotion over silica supported MoO_x when co-feeding 4MEs. Kinetic studies confirmed significant rate enhancements due to 4MEs co-feeding, demonstrating their impact on kinetically relevant steps beyond the traditional Chauvin cycle. Steady-state titrations primarily attributed these effects to an increased density of active sites. NAP-XPS data indicated that 4MEs facilitate the reduction of Mo species to the more catalytically active Mo (IV) state. Furthermore, FTIR spectroscopy revealed additional factors influencing steady-state reactivity, indicating the greater likelihood of 4MEs interacting with surface Si-OH groups compared to propylene. The adsorption and desorption cycles of 4MEs generate free labile protons, enhancing active site formation through the 1,2-proton shift mechanism, which ultimately increases active site density.

The collective insights acquired from spectroscopy and kinetics support our hypothesis that the promotion effect in propylene self-metathesis arises from increased active site generation through the 1,2-proton shift mechanism in the presence of 4MEs. We propose a concurrent site renewal and decay mechanism, operating alongside the traditional Chauvin cycle over heterogeneous supported catalysts, which accounts for the full reversibility of the promotion effect. In addition, the promotional effects in silica-supported MoO_x-IWI catalysts inversely correlate with Mo loading and MoO_3 crystallinity, suggesting it is more pronounced with dispersed molybdate species on the catalyst surface near Si-OH groups, rather than with crystalline Mo clusters, even at higher metal loadings.

Methods

Catalyst synthesis and characterization

The synthesis and characterization of the MoO_x/SiO_2 prepared via the surface organometallic chemistry method (1.5%MoO_x-SOMC) have been previously reported.[14,17] For MoO_x/SiO_2 catalysts synthesized via the incipient wetness impregnation methods (MoO_x-IWI), silica gel (Sigma-Aldrich, Davisil Grade 646, pore size 150 Å, 300 m^2/g) was used as the SiO_2 support. The silica gel was heated at 500 ºC (3 °C/min) for 3 hours under flowing air (60 mL/min, Airgas, dry air) and then sieved to ensure particle sizes ranged from 40-60 mesh. Ammonium molybdate tetrahydrate (Fluka, ≥99%) dissolved in water (4 mL, type 1, purified by Thermo Scientific, Barnstead Nanopure system) was used as the Mo precursor solution. The amount of Mo precursor depended on the target Mo loading. The precursor solution was added dropwise to 2.0 g of the silica support. The slurry was slowly stirred and dried at room temperature (6 hours). Then, it was further dried at 90 °C (1 °C/min) for 3 hours and calcined at 400 °C (1 °C/min) under flowing air (60 mL/min, Airgas, dry air) for 3 hours. After the calcination, the catalyst was sieved again to keep the particle size range from 40-60 mesh. The Mo loading of the catalysts was confirmed by inductively coupled plasma-optical emission spectrometry (ICP-OES). Surface areas and average pore size of the support and each catalyst were determined by N_2 physisorption at 77 K (Quantachrome, Autosorb iQ). Before N_2 dosing, samples were outgassed under vacuum for 4 h at 523 K. Surface areas were determined by BET analysis, and average pore diameters were determined from the DFT method.[51]

Reactivity studies

All gases used for the kinetic and spectroscopic studies were purified before the reactor or analysis chamber. Helium (Airgas, UHP) and propylene (Airgas, Electronic grade, >99.95%) were purified with home-built moisture traps containing 3Å molecular sieves (MilliporeSigma, 4-8 mesh) and pre-activated 5×3mm R3-11G tablets (Research Catalysts). Mass flow controllers (Brooks SLA5800 with a 0254 controller) manipulated their flow rates. The air supply was from house air which is sequentially purified with Wilkerson modular compressed air filter (McMaster-Carr), FID tower (NM Plus 1350 FID Tower, VICI DBS), and indicating moisture trap (Restek, 22014). The air flow rate was controlled by a flow meter (Omega Engineering, FLDA3222G).

Promoter (2,3-dimethyl-1-butene and 2,3-dimethyl-2-butene) was introduced to the reactor using a syringe pump station connected to a vaporizer, which was bypassed for unpromoted runs. The vaporizer was made of a Tee union (Swagelok, 1/8-inch, SS-200-3) with a capillary stainless-steel tubing (Sigma-Aldrich, 1/16-inch OD, 0.005-inch ID, 10 cm length). A PEEK tubing (McMaster, 51085K41) connected the syringe and vaporizer via a zero dead volume union (Idex H&S, P-704).

A 5 mL syringe (Hamilton, 1000) is connected to the PEEK tubing via a Luer adapter (Idex H&S, P-659) and a 10-32 coned fitting (F-120X). The syringe is controlled by a syringe pump (Masterflex, EW-74900-00) that can accurately deliver 0.15 mL/hour of promoter into the vaporizer. After the vaporizer, the gas phase promoter was purified with an additional home-built moisture trap.

The reactivity of each catalyst was tested in a U-shaped tubular reactor (SS304, 0.25 in. OD, 0.18 in. ID). The 1.5% MoO_x-SOMC catalyst was loaded inside an N_2-filled glovebox and sealed with two needle valves (Swagelok, SS-OKS2), whereas the incipient wetness impregnation catalysts were loaded outside the glovebox under standard atmospheric conditions. 10-30 mg of catalyst was mixed with 100 mg of inert SiC (Alfa Aesar, 46 grit, sieved to 40-60 mesh) to ensure a uniform bed. The mixture was sandwiched between two layers of 150 mg inert SiC and two quartz wool plugs (Technical Glass Products, 4-6 μm) inside the reactor. A K-type thermocouple (Omega Engineering) was placed touching the top of the catalyst bed. For 1.5% MoO_x-SOMC catalyst, both ends of the U-tube were fitted with needle valves (Swagelok), and the packed reactor was transferred out of the glovebox.

The reactor setup was leak-checked for each experiment. For a standard pretreatment procedure, the catalyst was heated to 400 °C (1 °C/min for MoO_x-SOMC and 3°C/min for MoO_x-IWI) for 3 hours and cooled to 270 °C under flowing air (50 mL/min). Then, the catalyst was purged at 270 °C for 30 mins and activated at 500 °C (2 °C/min) for 3 hours under flowing helium (100 mL/min). After the pretreatment, the catalyst was cooled to reaction temperature under flowing helium (50 mL/min) and switched to reaction conditions after the temperature inside the reactor stabilized. Heating was provided by a home-built furnace. The heating element was a high temperature, dual-element heating tape (Omega Engineering) wrapping around a tube (SS304, 2-1/2 inch OD, 2 inch ID, 6 inch Long). The heating element was packed with a 1-1/2 inch thick ceramic fiber insulation sheet (McMaster-Carr) and an aluminum sheet (McMaster-Carr) to maintain an isothermal condition. The furnace was controlled by a temperature controller (Cole-Parmer, Digi-Sense 89000). Transfer lines from the moisture trap to the reactor outlet were heat traced to > 85 °C. The reactor effluent was analyzed with gas chromatography (Shimadzu GC-2014) equipped with an Agilent HP-PLOT Al_2O_3-S (30 m × 0.25 mm) column and a flame ionization detector. Reaction effluent was periodically collected in a gas bag and analyzed using a GC–MS system (Agilent 7820A + 5977B MSD). The flow rates of all products were quantified by means of the flame ionization detector calibrated against known standards.

All rates reported were at a steady state. We defined the rate of propylene metathesis as the sum of production rates of ethylene, trans-2-butene, and cis-2-butene. The background reactivity of the reactor system was considered with an empty reactor solely consisting of the inert SiC and SiO_2. We observed no ethylene, trans-2-butene, and cis-2-butene with trace amounts of C_6 olefins at 200 ^oC. The mass normalized rate was calculated according to Eq. 1. The carbon balance of all data closes within the expected uncertainties of the total flow rates.

$$r = \frac{\sum F_i}{m_{cat}} \qquad \text{(Eq. 1)}$$

In Eq. 1, r is the catalyst mass normalized rate; F_i is the molar flow rate of product i; m_{cat} is the mass of the catalyst.

Steady state transient active site titration

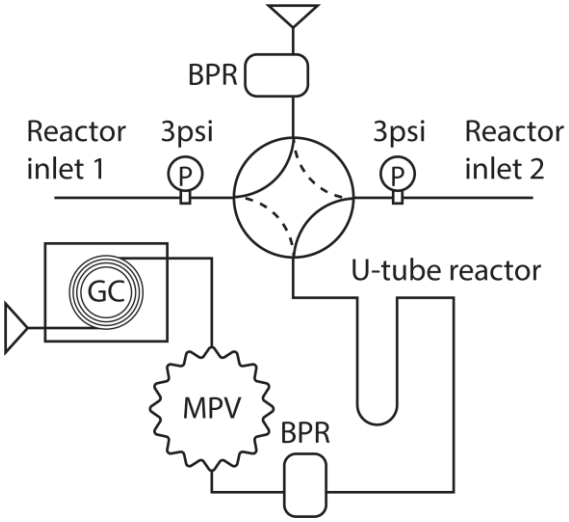

Figure 7. A simple scheme for the steady-state isotopic transient kinetic analysis reactor.

Steady state transient active site titration was performed using a steady-state isotopic transient kinetic analysis reactor **(Fig. 7)**, specifically chosen to minimize flow fluctuations during titration. Reactants, promoters, and carrier helium were purified and delivered the same way as in the reactivity studies. The pressure of the two reactor inlets was kept at 3 psi with two back pressure regulators (BPR). For these experiments, 20-30 mg of catalysts were loaded into a U-tube reactor. The catalysts underwent pretreatment identical to that used in our reactivity studies. Since supported metal oxides do not inherently possess metal alkylidene structures, recognized as the active sites for olefin metathesis, we subjected the pretreated catalysts to 20% 2-butenes balanced with helium at 180 °C to generate surface Mo oxo ethylidene. This specific condition was sustained for at least 14 hours to guarantee achieving a steady state.

For titrating surface Mo oxo ethylidene, we altered the reactor feed to consist of 20% ethylene in helium, which produced both propylene and Mo oxo methylidene. During this stage, we captured the reactor effluent in 16 loops of multi-position valves (MPV) for subsequent analysis using the same online GC employed in our reactivity tests. The titration results revealed a notable tailing peak in propylene production **(Supplementary Fig. S4B)**, involving both the propylene generated directly from the Mo oxo ethylidene titration and the propylene resulting from the cross-metathesis of ethylene and 2-butenes. To accurately discern the contribution of each component to the overall propylene production, a series of titration experiments were conducted at varying total flow rates **(Supplementary Fig. S4C and D)**. We graphed the propylene production at each flow rate as a function of space time. By extrapolating the propylene production to zero space time (y-intercept), we estimated the propylene production corresponding to an infinite total flow rate. This extrapolation method effectively minimized the influence of 2-butenes holdup, thereby reducing the contribution of ethylene and 2-butene cross-metathesis to the final Mo oxo ethylidene counts.

NAP-XPS characterization:

The typical catalyst pretreatment was applied to all catalysts. After activation under flowing helium at 500 ºC, the catalyst was cooled to room temperature, exposed to the ambient environment, and stored in clean glass vials. For NAP-XPS experiments, the catalyst powders were pressed into a thin pellet on a Cu foil and loaded into the analysis chamber. Before the reaction, the catalyst pellet was heated at 300 ºC (~6 ºC/min, held for 30 mins) and then cooled to 250 ºC under UHV (10^{-8} mbar). The heating was performed with an infrared laser and monitored with a K-type thermocouple.

The NAP-XP spectra were acquired at the Center for Functional Nanomaterials at Brookhaven National Laboratory.[52] The instrument was manufactured by SPECS Surface Nano Analysis GmbH and is equipped with a monochromated Al anode (1486.7 eV) focused to a spot size of ~300 microns, a PHIOBOS 150 NAP hemispherical analyzer and lens system, and a 1D-delay line

detector. The aperture separating the analysis chamber from the lens system was 300 microns, and the sample to aperture distance was 600 microns. Propylene and 2,3-dimethyl-1-butene i4ME were dosed via precision leak valves. NAP-XPS spectra were obtained under four conditions: 0.48 mbar C_3H_6; 0.48 mbar C_3H_6 with 0.12 mbar i4ME; 0.48 mbar C_3H_6 with 0.24 mbar i4ME; and 0.48 mbar C_3H_6 with 0.48 mbar i4ME (C_3H_6 : i4ME = 4 : 1, 2 : 1, and 1 : 1). The spectra showing Mo3d peaks are accumulations of 15-20 scans. Peak shifts associated with surface charging are corrected by referencing the adventitious C 1s core level to 284 eV and Si $2p_{3/2}$ core level to 104 eV. The spectra were fitted with CasaXPS using Gaussian/Lorentzian functional (60:40) and the Shirley-type background.[33,53]

In-situ DR UV-Vis characterization

In-situ DR UV-Vis spectra were acquired using a Cary 5000 UV-Vis-NIR spectrophotometer. All UV-Vis spectra were collected relative to a baseline of $BaSO_4$ measured under ambient conditions. The catalyst powders were loaded into the sample holder and placed into the DiffusIR environmental chamber (PIKE Technologies, 162-4200). Before experiments, the catalyst powders were calcined to 400 °C (1 °C/min for SOMC catalyst, 3 °C/min otherwise, held for 3 hours) under flowing dry air (50 mL/min) for 3 hours then cooled under flowing air to 300 °C. For edge energy, the catalyst powders were continuously cooled under flowing air to 50 °C.

For the in-situ propylene metathesis study, the catalyst powders were further purged under flowing helium (100 mL/min) at 300 °C for 30 mins and activated under flowing helium at 500 °C (2 °C/min) for 3 h. Then, the catalyst powders were cooled to 250 ºC. A typical reaction condition was 10% propylene with 1% 4MEs as the promoter in a helium balance with a 50 mL/min total flow rate.

The reflectance spectra from UV-Vis spectroscopy were converted to Kubelka-Munk Function using Eq. 2. The edge energy for allowed transitions was the y-intercept of a straight line fitted at the low-energy rise of a plot of $[F(R_\infty)h\upsilon]^2$ as a function of $h\upsilon$ (photon energy).[54]

$$F(R_\infty) = \frac{(1-R_\infty)^2}{2 \cdot R_\infty} \qquad \text{(Eq. 2)}$$

In-situ FTIR characterization

In-situ IR spectra were acquired on a Bruker Vertex 70 spectrometer equipped with a liquid N_2 cooled Hg-Cd-Te (MCT) detector by averaging 128 scans at 4 cm^{-1} resolution and an aperture setting of 4 mm between 4000 and 400 cm^{-1}. All IR spectra were collected relative to an empty cell spectrum measured at 150 °C with 60 mL/min helium flowing after heating the empty cell to 400 °C for 3 h in purified house air. The 1.5%MoO_x-SOMC catalyst and the $SiO_{2\text{-}700}$ powder (7-10 mg) were pressed into 7 mm diameter wafers, placed in a stainless-steel sample holder (Harrick Scientific Products Inc.), and loaded into a high-temperature transmission IR cell (Harrick Scientific Products Inc.) sealed with KBr windows (32 x 3 mm; Harrick Scientific Products Inc.) and 2-way bellows sealed valves (Swagelok, SS-4H) inside the glovebox. The spectrometer and the space between the cell and the detector were continuously purged with dry N_2 (liquid N2 boil-off and passed through activated 3A molecular sieves) to remove background traces of CO_2 and H_2O. All reported IR spectra were baseline-corrected and normalized by the total area of the T-O-T combination and overtone modes (2100-1750 cm-1) of the parenting spectrum.

Before experiments, the 1.5%MoO_x-SOMC catalyst was heated to 400 °C (1 °C/min) under flowing air (50 mL/min) for 3 h, cooled under flowing air to 300 °C, purged under flowing helium (60 mL/min) for 60 mins, and then cooled under flowing helium to the desired temperature. To dose propylene, 20% of propylene in a helium balance (Airgas, UHP) was mixed with helium (Airgas, UHP) to provide 10% propylene. The promoter (4MEs) was dosed via a vaporizer identical to the one used in the reactor setup.

For the temperature programmed desorption of 4MEs, the catalyst pellet was first saturated with probe molecules at 50 °C. Then, the pellet was purged under flowing helium (100 mL/min) until the spectra were stabilized. Next, the catalyst pellet was heated to labeled temperatures (3 °C/min) under flowing helium (100 mL/min). The IR spectrum was continuously collected during the temperature ramping process.

The experimental setup and details for the adsorption of CD_3CN were described elsewhere.[55] After being heated to 400 °C (1 °C/min) under flowing air (50 mL/min) for 3 h and cooled under flowing air to 330 °C, the catalyst pellet was purged under flowing nitrogen (100 mL/min) for 60 mins, and further cooled under flowing nitrogen to 50 °C. The in-situ IR cell was evacuated to less than 0.02 Torr, and then, CD_3CN was introduced into the IR cell through the Schlenk line to reach a total pressure of 20.00 Torr. After 30 minutes, the catalyst pellet was purged under flowing nitrogen (100 mL/min) until steady state.

Raman characterization:

The Raman spectra were acquired using a Renishaw Invia Reflex Micro Raman equipped with a 532 nm laser. Prior to the spectral acquisition, samples (50-60 mg) were dehydrated ex-situ in a Raman High Temperature Reaction chamber (Harrick Scientific, HVC-MRA-5). Samples were calcined at 400 °C (1 °C/min for SOMC catalyst, 3 °C/min otherwise, held for 3 h) and cooled to room temperature under flowing purified house air (50 mL/min). Then, the cell was sealed using 2-way bellows sealed valves (Swagelok, SS-4H) and transferred into the Raman sample chamber. Spectra were obtained at a resolution of 2 cm^{-1} at room temperature using a laser power of 25 mW (5 mW for SOMC catalyst) with an accumulation of 32 scans.

AUTHOR INFORMATION

Corresponding Author

* Yuriy Román-Leshkov: yroman@mit.edu

ACKNOWLEDGMENTS

The MIT authors acknowledge the U.S. Department of Energy, Office of Basic Energy Sciences under Award DE-SC0016214 for the financial support as well as the National Science Foundation under CBET-1846426. This research used the Proximal Probes Facility of the Center for Functional Nanomaterials (CFN), which is a U.S. Department of Energy Office of Science User Facility, at Brookhaven National Laboratory under Contract No. DE-SC0012704. The authors acknowledge Griffin Drake and Xianyuan Wu for their feedback on the manuscript.

COMPETING INTERESTS

The authors declare no competing interests.

ADDITIONAL INFORMATION

Supplementary information is available online.

TOC:

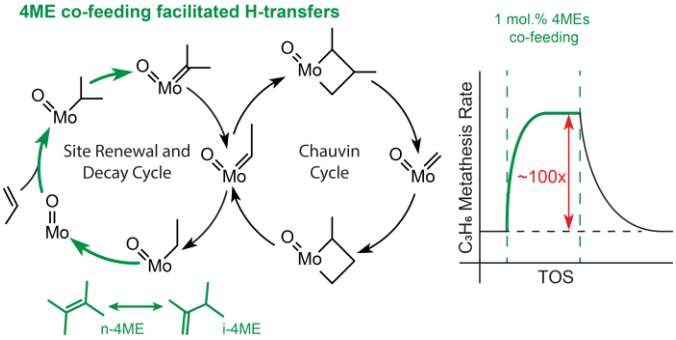

References:

1 Keim, W. Oligomerization of Ethylene to α - Olefins: Discovery and Development of the Shell Higher Olefin Process (SHOP). *Angewandte Chemie International Edition* **52**, 12492-12496 (2013).

2 Mol, J. Industrial applications of olefin metathesis. *Journal of Molecular Catalysis A: Chemical* **213**, 39-45 (2004).

3 Rouhi, A. M. Olefin metathesis: the early days. *Chem Eng News* **80**, 34-38 (2002).

4 Lwin, S. & Wachs, I. E. Olefin Metathesis by Supported Metal Oxide Catalysts. *ACS Catalysis* **4**, 2505-2520, doi:10.1021/cs500528h (2014).

5 Casey, C. P. & Burkhardt, T. J. Reactions of (diphenylcarbene) pentacarbonyltungsten (0) with alkenes. Role of metal-carbene complexes in cyclopropanation and olefin metathesis reactions. *Journal of the American Chemical Society* **96**, 7808-7809 (1974).

6 Jean - Louis Hérisson, P. & Chauvin, Y. Catalyse de transformation des oléfines par les complexes du tungstène. II. Télomérisation des oléfines cycliques en présence d'oléfines acycliques. *Die Makromolekulare Chemie: Macromolecular Chemistry and Physics* **141**, 161-176 (1971).

7 Hoveyda, A. H. & Zhugralin, A. R. The remarkable metal-catalysed olefin metathesis reaction. *Nature* **450**, 243 (2007).

8 Amakawa, K. *et al.* In situ generation of active sites in olefin metathesis. *Journal of the American Chemical Society* **134**, 11462-11473, doi:10.1021/ja3011989 (2012).

9 Howell, J. G., Li, Y.-P. & Bell, A. T. Propene metathesis over supported tungsten oxide catalysts: A study of active site formation. *ACS Catalysis* **6**, 7728-7738 (2016).

10 Mougel, V. *et al.* Low Temperature Activation of Supported Metathesis Catalysts by Organosilicon Reducing Agents. *ACS central science* **2**, 569-576 (2016).

11 Gani, T. Z. *et al.* Promoting active site renewal in heterogeneous olefin metathesis catalysts. *Nature* **617**, 524-528 (2023).

12 Liu, S., Boudjelel, M., Schrock, R. R., Conley, M. P. & Tsay, C. Interconversion of Molybdenum or Tungsten d2 Styrene Complexes with d0 1-Phenethylidene Analogues. *Journal of the American Chemical Society* **143**, 17209-17218 (2021).

13 Amakawa, K. *et al.* In situ generation of active sites in olefin metathesis. *Journal of the American Chemical Society* **134**, 11462-11473 (2012).

14 Yamamoto, K. *et al.* Silica-supported isolated molybdenum di-oxo species: formation and activation with organosilicon agent for olefin metathesis. *Chemical Communications* **54**, 3989-3992 (2018).

15 Copéret, C. *et al.* Olefin metathesis: what have we learned about homogeneous and heterogeneous catalysts from surface organometallic chemistry? *Chemical science* **12**, 3092-3115 (2021).

16 Amakawa, K. *et al.* Active sites in olefin metathesis over supported molybdena catalysts. *ChemCatChem* **7**, 4059-4065 (2015).

17 Berkson, Z. J. *et al.* Active Site Descriptors from 95Mo NMR Signatures of Silica-Supported Mo-Based Olefin Metathesis Catalysts. *Journal of the American Chemical Society* (2023).

18 Berkson, Z. J. *et al.* Olefin-surface interactions: a key activity parameter in silica-supported olefin metathesis catalysts. *JACS Au* **2**, 777-786 (2022).

19 Skoda, D. *et al.* Propylene Metathesis over Molybdenum Silicate Microspheres with Dispersed Active Sites. *ACS catalysis* **13**, 12970-12982 (2023).

20 Grünert, W. *et al.* Reduction and metathesis activity of MoO3/Al2O3 catalysts II. The activation of MoO3/Al2O3 catalysts. *Journal of Catalysis* **135**, 287-299 (1992).

21 Chatterjee, A. K., Choi, T.-L., Sanders, D. P. & Grubbs, R. H. A general model for selectivity in olefin cross-metathesis. *Journal of the American Chemical Society* **125**, 11360-11370 (2003).

22 Zhang, Q., Xiao, T., Liu, C., Otroshchenko, T. & Kondratenko, E. V. Performance Descriptors for Catalysts Based on Molybdenum, Tungsten, or Rhenium Oxides for Metathesis of Ethylene with 2 - Butenes to Propene. *Angewandte Chemie International Edition*, e202308872 (2023).

23 Ding, K. *et al.* Highly efficient activation, regeneration, and active site identification of oxide-based olefin metathesis catalysts. *ACS Catalysis* **6**, 5740-5746 (2016).

24 Zhang, B., Xiang, S., Frenkel, A. I. & Wachs, I. E. Molecular Design of Supported MoO x Catalysts with Surface TaO x Promotion for Olefin Metathesis. *Acs Catalysis* **12**, 3226-3237 (2022).

25 Kondratenko, V. A., Hahn, T., Bentrup, U., Linke, D. & Kondratenko, E. V. Metathesis of ethylene and 2-butene over MoOx/Al2O3-SiO2: Effect of MoOx structure on formation of active sites and propene selectivity. *Journal of Catalysis* **360**, 135-144 (2018).

26 Chakrabarti, A. & Wachs, I. E. Molecular Structure–Reactivity Relationships for Olefin Metathesis by Al2O3-Supported Surface MoO x Sites. *ACS Catalysis* **8**, 949-959 (2018).

27 Wulfers, M. J., Tzolova-Müller, G., Villegas, J. I., Murzin, D. Y. & Jentoft, F. C. Evolution of carbonaceous deposits on H-mordenite and Pt-doped H-mordenite during n-butane conversion. *Journal of catalysis* **296**, 132-142 (2012).

28 Dong, J. *et al.* Ultrathin two-dimensional porous organic nanosheets with molecular rotors for chemical sensing. *Nature Communications* **8**, 1142 (2017).

29 Chan, K. W. *et al.* C–H Activation and Proton Transfer Initiate Alkene Metathesis Activity of the Tungsten (IV)–Oxo Complex. *Journal of the American Chemical Society* **140**, 11395-11401 (2018).

30 Amakawa, K. *et al.* How strain affects the reactivity of surface metal oxide catalysts. *Angewandte Chemie International Edition* **52**, 13553-13557 (2013).

31 Wu, J. F. *et al.* Enhanced Olefin Metathesis Performance of Tungsten and Niobium Incorporated Bimetallic Silicates: Evidence of Synergistic Effects. *ChemCatChem* **12**, 2004-2013 (2020).

32 Myradova, M. *et al.* Tuning the metathesis performance of a molybdenum oxide-based catalyst by silica support acidity modulation and high temperature pretreatment. *Catalysis Science & Technology* **12**, 2134-2145 (2022).

33 Michorczyk, P., Wegrzyniak, A., Wegrzynowicz, A. & Handzlik, J. Simple and efficient way of molybdenum oxide-based catalyst activation for olefins metathesis by methane pretreatment. *ACS Catalysis* **9**, 11461-11467 (2019).

34 Seman, M., Kondo, J., Domen, K., Radhakrishnan, R. & Oyama, S. Reactive and inert surface species observed during methanol oxidation over silica-supported molybdenum oxide. *The Journal of Physical Chemistry B* **106**, 12965-12977 (2002).

35 Ghosh, A. K. & Kydd, R. A. A Fourier-transform infrared spectral study of propene reactions on acidic zeolites. *Journal of Catalysis* **100**, 185-195 (1986).

36 Hadjiivanov, K. in *Advances in Catalysis* Vol. 57 99-318 (Elsevier, 2014).

37 Chakarova, K., Drenchev, N., Mihaylov, M., Nikolov, P. & Hadjiivanov, K. OH/OD isotopic shift factors of isolated and H-bonded surface silanol groups. *The Journal of Physical Chemistry C* **117**, 5242-5248 (2013).

38 Gabrienko, A. A. *et al.* Direct measurement of zeolite Brønsted acidity by FTIR spectroscopy: solid-state 1H MAS NMR approach for reliable determination of the integrated molar absorption coefficients. *The Journal of Physical Chemistry C* **122**, 25386-25395 (2018).

39 Pelmenschikov, A., Van Santen, R., Janchen, J. & Meijer, E. Acetonitrile-d3 as a probe of Lewis and Broensted acidity of zeolites. *The Journal of Physical Chemistry* **97**, 11071-11074 (1993).

40 Tuma, C. & Sauer, J. Protonated isobutene in zeolites: tert‐butyl cation or alkoxide? *Angewandte Chemie International Edition* **44**, 4769-4771 (2005).

41 Freundlich, J. S., Schrock, R. R., Cummins, C. C. & Davis, W. M. Organometallic Complexes of Tantalum That Contain the Triamidoamine Ligand,[(Me3SiNCH2CH2) 3N] 3-, Including an Ethylidene Complex Formed via a Phosphine-Catalyzed Rearrangement of an Ethylene Complex. *Journal of the American Chemical Society* **116**, 6476-6477 (1994).

42 Hirsekorn, K. F. *et al.* Thermodynamics, Kinetics, and Mechanism of (silox) 3M (olefin) to (silox) 3M (alkylidene) Rearrangements (silox= tBu3SiO; M= Nb, Ta). *Journal of the American Chemical Society* **127**, 4809-4830 (2005).

43 Liu, S., Schrock, R. R., Conley, M. P., Tsay, C. & Carta, V. An Exploration of the Acid-Catalyzed Interconversion of Mo (NAr)(CR1R2)(OR) 2 Complexes and Their Mo (NAr)(Olefin)(OR) 2 Isomers (Ar= 2, 6-i-Pr2C6H3, OR= OSiPh3 or OAr). *Organometallics* **42**, 2251-2261 (2023).

44 Liu, S., Conley, M. P. & Schrock, R. R. Synthesis of Mo (IV) para-Substituted Styrene Complexes and an Exploration of Their Conversion to 1-Phenethylidene Complexes. *Organometallics* (2022).

45 Handzlik, J., Kurleto, K. & Gierada, M. Computational Insights into Active Site Formation during Alkene Metathesis over a MoO x/SiO2 Catalyst: The Role of Surface Silanols. *ACS Catalysis* **11**, 13575-13590 (2021).

46 Chan, K. W., Mance, D., Safonova, O. V. & Copéret, C. Well-defined silica-supported tungsten (IV)–oxo complex: olefin metathesis activity, initiation, and role of Brønsted acid sites. *Journal of the American Chemical Society* **141**, 18286-18292 (2019).

47 Song, Y., Zhu, X. & Xu, L. Study on the process of transformation of olefin into aromatics over HZSM-5. *Catalysis Communications* **7**, 218-223 (2006).

48 Sassi, A., Wildman, M. A. & Haw, J. F. Reactions of butylbenzene isomers on zeolite HBeta: methanol-to-olefins hydrocarbon pool chemistry and secondary reactions of olefins. *The Journal of Physical Chemistry B* **106**, 8768-8773 (2002).
49 Plessow, P. N., Enss, A. E., Huber, P. & Studt, F. A new mechanistic proposal for the aromatic cycle of the MTO process based on a computational investigation for H-SSZ-13. *Catalysis Science & Technology* **12**, 3516-3523 (2022).
50 Collett, C. & McGregor, J. Things go better with coke: the beneficial role of carbonaceous deposits in heterogeneous catalysis. *Catalysis Science & Technology* **6**, 363-378 (2016).
51 Landers, J., Gor, G. Y. & Neimark, A. V. Density functional theory methods for characterization of porous materials. *Colloids and Surfaces A: Physicochemical and Engineering Aspects* **437**, 3-32 (2013).
52 Eads, C. N. *et al.* Multi-modal surface analysis of porous films under operando conditions. *Aip Advances* **10**, doi:10.1063/5.0006220 (2020).
53 Murugappan, K. *et al.* Operando NAP-XPS unveils differences in MoO3 and Mo2C during hydrodeoxygenation. *Nature Catalysis* **1**, 960-967 (2018).
54 Tian, H., Roberts, C. A. & Wachs, I. E. Molecular structural determination of molybdena in different environments: Aqueous solutions, bulk mixed oxides, and supported MoO3 catalysts. *The Journal of Physical Chemistry C* **114**, 14110-14120 (2010).
55 Di Iorio, J. R., Johnson, B. A. & Román-Leshkov, Y. Ordered hydrogen-bonded alcohol networks confined in Lewis acid zeolites accelerate transfer hydrogenation turnover rates. *Journal of the American Chemical Society* **142**, 19379-19392 (2020).